SUPPLEMENTARY INFORMATION

Detection of nanoaggregates in highly concentrated strongly absorbing colloids without sample dilution

S. Bali[1]*, J. T. Boivin[2], R. N. M. Ducay[1], N. Philip[1], J. D. Brinton[1], L. M. Bali[1], J. P. Scaffidi[3], and J. A. Berberich[2]*

[1]Department of Physics, Miami University, Oxford, OH 45056
[2]Department of Chemical, Paper and Biomedical Engineering, Miami University, Oxford, OH 45056
[3]Scaffidi Scientific Consulting, Philadelphia, PA 19144
*Corresponding authors: balis@miamioh.edu, berberj@miamioh.edu

S-I: Preparation of functionalized gold nanoparticles

Gold nanoparticles (AuNPs) were prepared by the Lee-Meisel citrate reduction procedure, as follows. Briefly, 240 mg hydrogen tetrachloroaurate (Alfa Aesar, Ward Hill, MA) was dissolved in 500 mL 18.2 MΩ DI water. The solution was brought to a boil, and 50 mL 18.2 MΩ DI water containing 1.0 % w/v tri-sodium citrate (VWR, Radnor, PA) was added. The reaction mixture was allowed to boil for an hour, and the resulting wine-red solution was rapidly cooled to room temperature.

Carboxylic acid functionality was added to the AuNPs by adding 400 µL 3-mercaptopropionic acid ("MPA", Alfa Aesar) to 40 mL of the cooled AuNP solution, and reacting for one hour under bath sonication. Excess MPA was removed via triplicate centrifugation, and the MPA-functionalized AuNPs particles were re-dispersed in 18.2 MΩ DI water by tip sonication.

S-II: Cleaning the glass cover slip above the prism

The coverslips are prepared by cleaning in Piranha solution (75mL of concentrated sulfuric acid and 25 mL of 30% w/v hydrogen peroxide) for 20 minutes and then rinsing thoroughly with deionized water before drying with ultra-high purity nitrogen.

S-III: Measurement of reflectance profiles from our sensor shown in Fig. 1(b)

First, we measure the reflected intensity profile with no sample - this yields I_i (θ_i) provided TIR occurs at the coverslip-air interface for all θ_i . The measurement is repeated 100 times, and an average profile is generated - this process takes 10 s. Next, the sample is placed on

the coverslip, and the average reflected intensity profile is similarly generated, yielding $I_r\ (\theta_i)$. Finally, the ratio of the two profiles is taken, yielding $I_r\ /\ I_i\ (\theta_i)$, for which each datapoint in Fig. 1(b) is represented by a gray dot. The standard deviation on each datapoint is smaller than the dot size.

S-IV: Characterization of aggregated NPs by alternative methods

UV-Vis absorption spectra (Agilent model 8453 spectrophotometer, Santa Clara, CA) of the AuNP solutions were recorded. In addition, DLS and zeta potential measurements (Zeta-Plus, Brookhaven Instruments, Holtsville, NY) were performed on the aggregated solutions at room temperature. For DLS particle sizing, the samples were diluted 1:200 in the aggregation buffer for analysis. For zeta potential measurement, samples were diluted 1:20. For UV-Vis, DLS, and zeta potential measurements, the sample was allowed to sit in the instrument for 30 min after addition of the aggregation-inducing agent before recording data, to ensure sufficient settling of aggregates has occurred Interestingly, the sample placed in the UV-Vis spectrophotometer cuvette was identical to the sample placed on top of the glass prism of our sensor, i.e., no sample dilution was performed for the UV-Vis data. This was because, upon aggregation, the sample effectively underwent a large "dilution" as explained in S-V below.

Fig. S1 shows zeta potential measurements which indicate that pH-induced (and ionic strength induced) aggregation occurs at HCl (and NaCl) concentrations in accordance with the TIR, UV-Vis, and DLS measurements in Fig. 3. Zeta potentials of approximately 0 to ±5 mV imply suppression of surface charge, causing attractive Van der Waal forces to dominate over repulsive electrostatic forces, enabling rapid aggregation. Zeta potentials of approximately ±20 to 25 mV imply the presence of sufficient surface charge to prevent aggregation.

In the case of HCl, the negative charges from the propionic acid in the MPA-functionalized AuNPs become increasingly protonated with increase in HCl concentration, causing the zeta potential to drop in magnitude to 5 mV at 0.4 mM (pH = 3.4). In the case of NaCl, the ionic strength-induced neutralization of the negatively charged carboxylic acid surface charge by charge-charge shielding resulting from the increasing concentration of ions in solution, causes the zeta potential magnitude to drop to ∼15 mV at 40 mM.
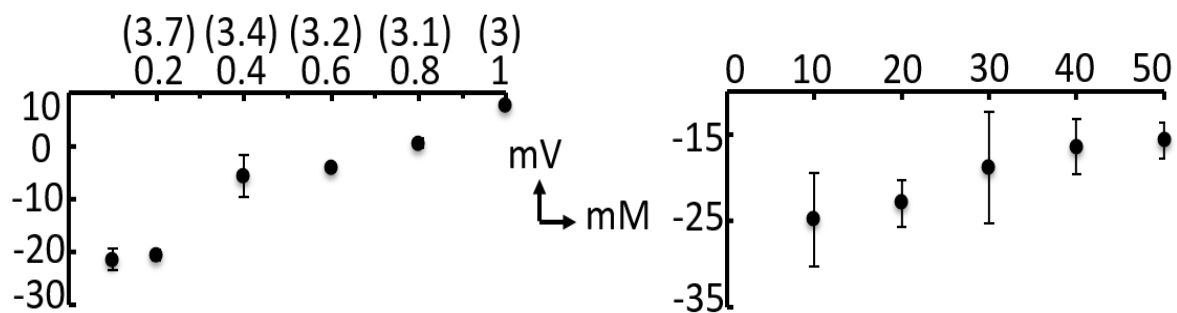
Figure S1: Zeta Potential of aggregated AuNP suspensions due to change in (left) pH, by adding HCl, or (right) ionic strength, by adding NaCl. The TIR, UV-Vis and DLS data for each condition is shown in Fig. 3.

S-V: Aggregation-induced settling: Effective sample dilution in UV-Vis spectrophotometry

Figs. S2 (a) and (b) show plots of AuNP attenuation coefficient α versus concentrations of (a) HCl and (b) NaCl, taken at two fixed time points: 15 minutes (red) and 30 minutes (blue). Solid lines correspond to α values measured by our TIR sensor while dashed lines correspond to α values measured by the spectrophotometer at the same wavelength as our laser source (see Sec. B.1). We see that our sensor and the spectrophotometer agree on the concentration at which the onset of aggregation occurs: There is a significant increase in attenuation when the HCl concentration passes 0.2 mM and the NaCl concentration passes 30 mM.
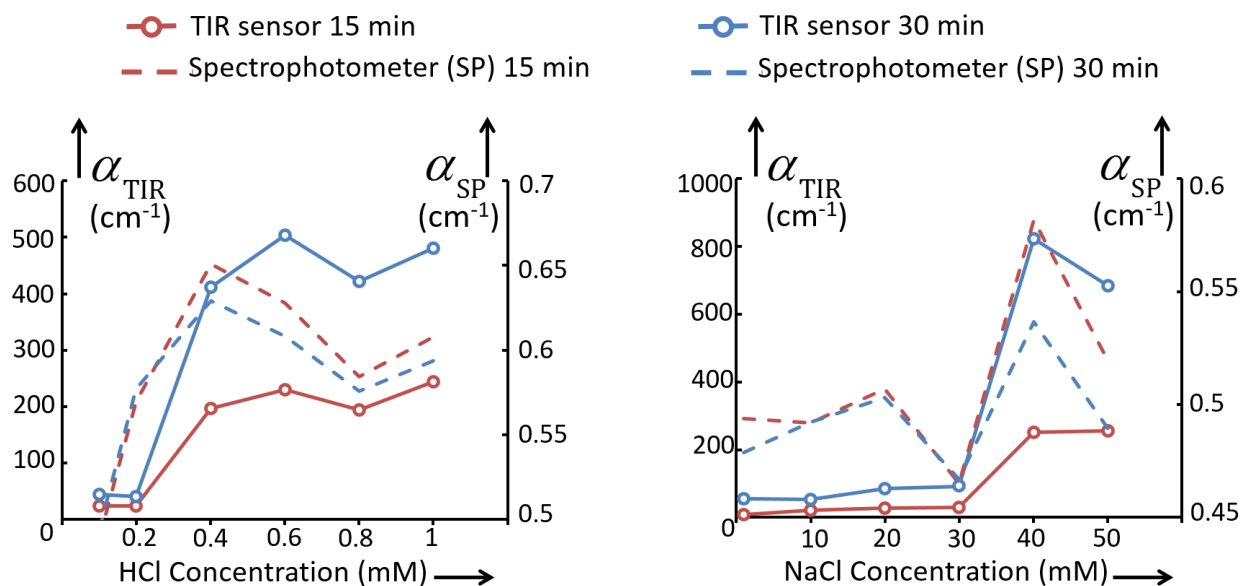

Figure S2: Attenuation coefficient α (in cm^{-1}) for the AuNP suspensions versus concentrations of (a) HCl and (b) NaCl as the aggregation-inducing agent, at fixed time-points of 15 min (red) and 30 min (blue), as measured by our TIR sensor (solid lines) and the UV-Vis spectrophotometer at the same wavelength (dashed lines). Both TIR and UV-Vis sensors agree that the effects of aggregation-induced settling are apparent once the concentration exceeds 0.2 mM HCl and is $\geq$ 30 mM NaCl. At concentrations where significant aggregation occurs, the TIR sensor shows an increase in attenuation from 15 minutes to 30 minutes, while the spectrophotometer sees a corresponding decrease in attenuation – for explanation see text below and Fig. S2.

However, when we look at the attenuation coefficients from the spectrophotometer and our sensor (dashed and solid lines respectively) at two fixed time intervals, 15 mins and 30 mins, we notice that the spectrophotometer attenuation coefficients decrease over time while our sensor's coefficients increase. This is due to the fact that the spectrophotometer is seeing a region of the sample in the center of a cuvette which aggregated particles are exiting as they settle at the

bottom, while the TIR sensor is sensitive to aggregated particles that sink and enter into the wavelength-sized sample layer located just above the coverslip sitting on top of the prism. Over time, this behavior causes the α values to decrease in the spectrophotometer and to increase in our sensor, as shown in Fig. S2 (a) and (b) below.

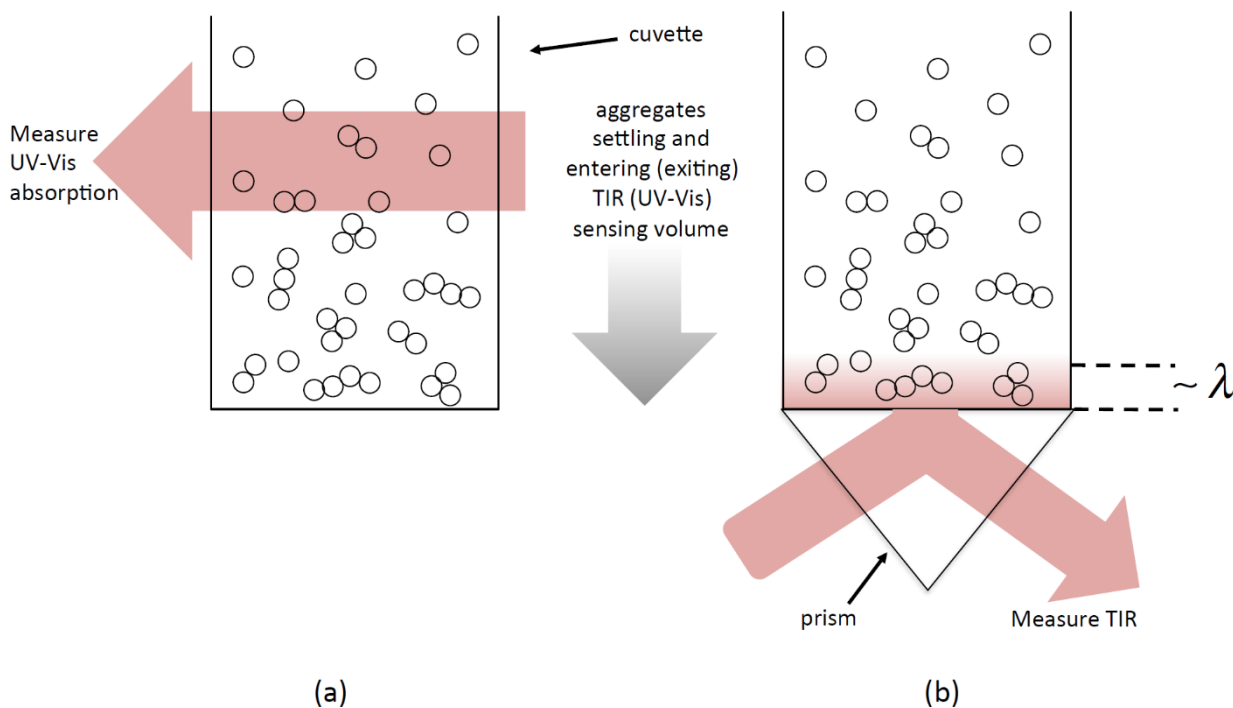(a)   (b)

Figure. S3: An illustration (not to scale) of how the aggregated particles settle over time. They a) exit the irradiating beam used in the UV-Vis spectrophotometer, leading to a decrease in the measured absorbance, hence also a decrease in the attenuation coefficient α, and b) enter the wavelength-sized sample layer located just above the TIR sensor, leading to an increase in the measured attenuation coefficient α.